Journal of Electroceramics, 13, 149–154, 2004

Integration of MgO on Si(001) Using SrO and $SrTiO_3$ Buffer Layers by Molecular Beam Epitaxy

F. NIU, A. MEIER* & B.W. WESSELS

Department of Materials Science and Engineering and Materials Research Center, Northwestern University, Evanston, IL 60208-3108, USA

Submitted February 13, 2003; Revised February 13, 2004; Accepted April 27, 2004

Abstract. Epitaxial MgO was deposited onto Si(001) substrates by molecular beam epitaxy using elemental metallic sources and molecular oxygen at temperatures from 150 to 400°C. To facilitate epitaxy through misfit strain relaxation, epitaxial MgO layers were grown on SrO and $SrTiO_3$ buffer layers deposited on Si(001) substrates. The structure of the epitaxial layers was determined by X-ray diffraction, reflection high-energy electron diffraction and transmission electron microscopy. The observed orientation for the MgO/SrO/Si multilayer is cube-on-cube. The X-ray rocking curve full width half maximum of the MgO on SrO buffer layers was 2.2°. $SrTiO_3$ buffer layers grown by recrystallization were epitaxial and exhibited improved morphology relative to those grown at a fixed growth temperature. X-ray analysis of a 5.2 nm recrystallized $SrTiO_3$ film indicates a fully relaxed and phase pure film. The observed orientation of MgO using $SrTiO_3$ buffer layers is MgO[100]||$SrTiO_3$[100]||Si[110].

Keywords: MgO, SrO, Si, $SrTiO_3$, epitaxy

Introduction

MgO is a good candidate for integration of ferroelectrics on silicon for opto-electronic integrated circuits owing to its low refractive index and excellent microwave properties. However, the large lattice mismatch between Si(001) and MgO makes direct epitaxial growth of MgO on Si difficult. Nevertheless, direct deposition of MgO on Si has been reported by a number of investigators despite a lattice mismatch of -29% for a fully commensurate cube-on-cube orientation of MgO on Si(001)[1–3]. To reduce the interfacial strain and facilitate epitaxy, epitaxial MgO has been deposited on Si using buffer layers. Using MOMBE, Niu et al. have deposited epitaxial MgO on Si(001) substrates with β-SiC buffer layers [4]. Sharma et al. have deposited epitaxial MgO on Si(001) with TiN buffer layers by pulsed laser deposition (PLD) [5].

In this study, the use of SrO and $SrTiO_3$ buffer layers for the deposition of MgO on Si(001) was investigated. In choosing these buffer layers, the possible epitaxial orientations and associated lattice mismatches were considered. The lattice mismatch for SrO on Si(001) with a cube-on-cube orientation is -5.6%. The cube-on-cube orientation and the SrO(110)||Si(001) with SrO[001]||Si[110] orientation are the only orientations reported for SrO on Si(001) [6–8]. A $SrTiO_3$ buffer layer with an orientation of $SrTiO_3$[110]||Si[100] has a $+1.7\%$ lattice mismatch. MgO with a cube-on-cube orientation on SrO has a lattice mismatch of $+22.5\%$ for commensurate films. For a 6:5 coincident epitaxy however, in this same orientation the misfit is just $+1.7\%$ and the cube-on-cube orientation has been reported for SrO deposited on MgO(001) substrates [9]. In the present study epitaxial MgO has been deposited on Si(001) using either a SrO or a $SrTiO_3$ buffer layer. The observed orientations were Si[100]||SrO[100]||MgO[100] and Si[110]||STO[100]||MgO[100] for MgO integrated using SrO and $SrTiO_3$ buffer layers, respectively.

Experimental

All films were grown in a molecular beam epitaxy system operating at a base pressure of $\sim 10^{-10}$ Torr.

*To whom all correspondence should be addressed. E-mail: b-wessels@northwestern.edu

Elemental sources of Sr, Mg and Ti were deposited from effusion cells and molecular O_2 was used as the oxidant. All films were deposited on 3 inch P-doped Si(001) substrates. In situ RHEED was used to monitor the evolution of film structure. As received silicon wafers were UV ozone cleaned prior to loading into the MBE system. The native oxide was subsequently thermally decomposed by holding the Si wafers at 850°C until the RHEED pattern of a 2×1 Si surface reconstruction was observed. The stage temperature was then reduced to 700°C where ∼5 Å of Sr was deposited. The substrate was held at 700°C for an additional 10 minutes, during which time a submonolayer silicide formed, passivating the Si surface [10, 11].

SrO Buffer Layers

SrO was deposited on the sub-monolayer silicide at 150°C at an O_2 pressure of $\sim 4 \times 10^{-8}$ Torr. MgO was then deposited on this SrO buffer layer. The effects of growth temperature on the MgO films were examined with all other deposition parameters held constant. These included the use 6 nm SrO buffer layers and an O_2 partial pressure of 4×10^{-8} Torr during the investigation of the effect of MgO growth temperature on the epitaxial quality of the film.

$SrTiO_3$ Buffer Layers

$SrTiO_3$ buffer layers were grown on the submonolayer silicide by codepositing Sr and Ti with an O_2 pressure of 8×10^{-8} Torr at a fixed growth temperature of 700°C. $SrTiO_3$ buffer layers were also grown by recrystallization [12] involving an initial codeposition of Sr and Ti at 200°C with an O_2 pressure of 8×10^{-8} Torr. This was followed by an anoxic anneal at 700°C for 15 minutes. MgO was deposited at a growth temperature of 200°C on Si(001) using a $SrTiO_3$ buffer layer. The $SrTiO_3$ buffer layer used was deposited at a fixed growth temperature of 700°C.

Results & Discussion

SrO Buffer Layers

Epitaxial SrO was deposited on Si(001) at a substrate temperature of 150°C. RHEED patterns from a 6 nm epitaxial SrO buffer layer along the Si[110] azimuth indicate that the SrO buffer layers exhibit a

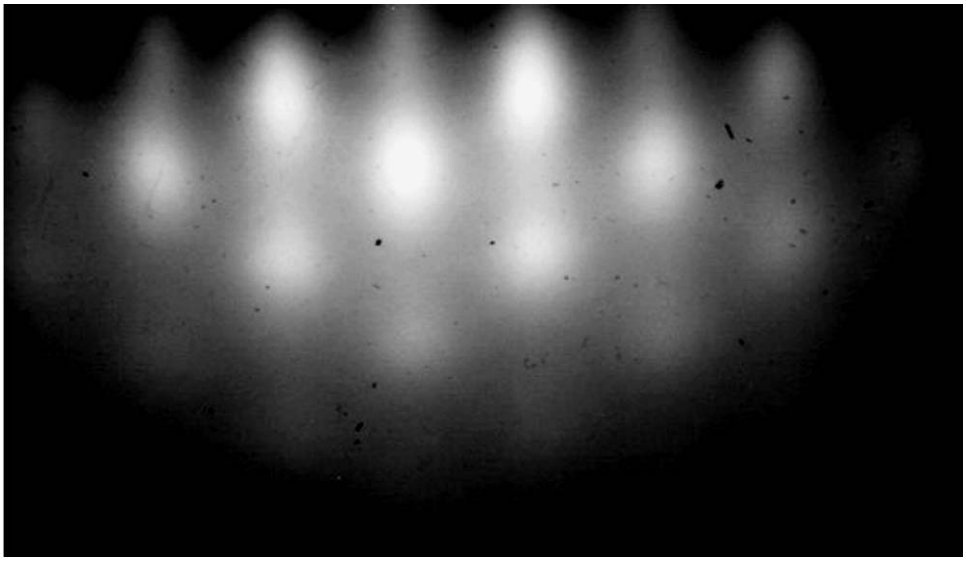

Fig. 1. RHEED Pattern of 6 nm SrO buffer layer along Si[110] azimuth. Orientation of SrO on Si is cube-on-cube and an epitaxial film exhibiting an island growth mode is evident.

cube-on-cube orientation with respect to the Si substrate. Additionally the RHEED patterns indicate that the SrO is growing in an island growth mode (Fig. 1). Epitaxial MgO was subsequently deposited on SrO buffer layers of 2.5 to 12 nm in thickness. SrO buffer layers of less than 2.5 nm resulted in a polycrystalline MgO overlayer. Furthermore, O_2 pressures from 4 to 12 $\times$ 10^{-8} Torr yielded epitaxial MgO overlayers while lower O_2 pressures resulted in two phases consisting of textured, polycrystalline MgO and an unidentified epitaxial phase.

Figure 2 shows the RHEED patterns for MgO films grown at different stage temperatures. The films exhibit a cube-on-cube orientation with respect to the Si(001) substrate. The epitaxial quality improved by increasing growth temperature from 25 to 300°C. In addition, the polycrystalline component became less prominent at higher growth temperatures. To improve epitaxy of MgO, a two step deposition process was used. A nominal five nanometer seed layer of MgO was deposited at 150°C followed by a ramp to 400°C where growth was continued. Figure 2(d) shows the RHEED pattern for a MgO film grown by this process. The film is free of any polycrystalline component as evidenced by the RHEED pattern. All the RHEED patterns in Fig. 2 are transmission-type RHEED patterns indicating a Volmer-Weber growth mode. The morphology seen in the AFM image (Fig. 3) likewise indicates an island growth mode. X-ray diffraction analysis of a 30 nm MgO film on a 12 nm SrO buffer layer indicated that the MgO film was fully relaxed. The FWHM of the MgO(002) rocking curve was 2.2°.

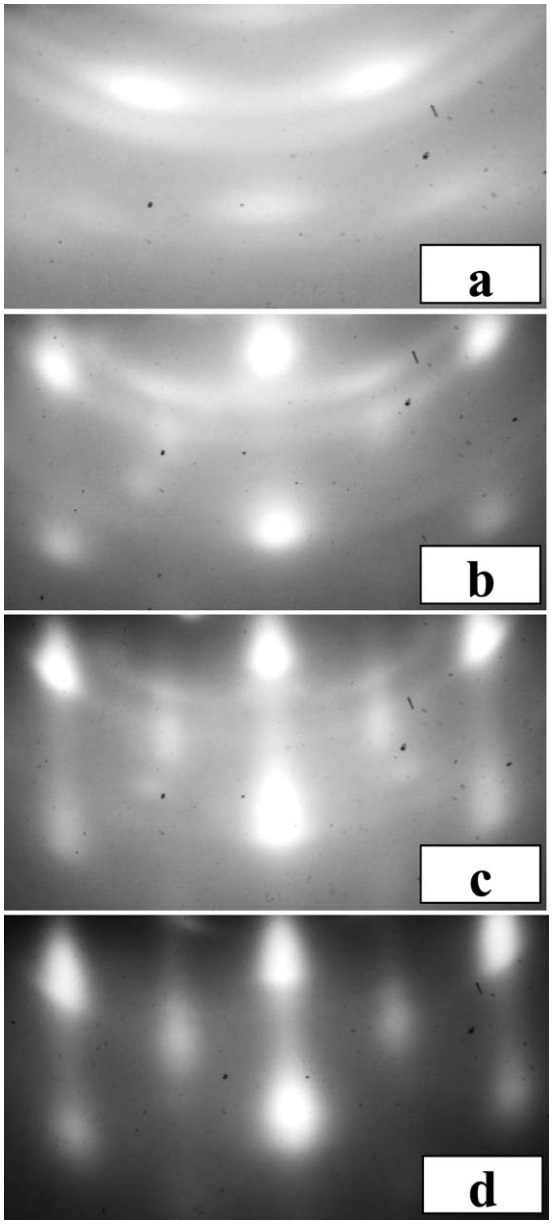

Fig. 2. MgO RHEED pattern for MgO deposition at (a) 25°C, (b) 150°C, (c) 300°C, and (d) by a two step growth process with an initial deposition of 5 nm at 150°C followed by continued deposition at 400°C. Epitaxy was achieved for deposition temperatures from 150 to 400°C.

$SrTiO_3$ Buffer Layers

Growth of epitaxial $SrTiO_3$ was studied using two different techniques. The first technique consisted of high temperature deposition of epitaxial $SrTiO_3$ on Si at 700°C. Growth under these conditions proceeded by Volmer-Weber island growth mode as indicated by both the RHEED pattern and the morphology seen in the AFM image (Fig. 4(a)). In contrast, for a $SrTiO_3$ film grown by recrystallization, Stranski-Krastanov layer-by-layer growth was indicated by both RHEED and AFM analysis. Four separate deposition and anneal cycles were employed. Figure 5(a) shows the RHEED pattern of a 6.5 Å $SrTiO_3$ film after the first deposition cycle. The RHEED pattern indicates a smooth, two dimensional epitaxial $SrTiO_3$ layer is established at the end of the first deposition cycle. Sequential RHEED patterns taken during

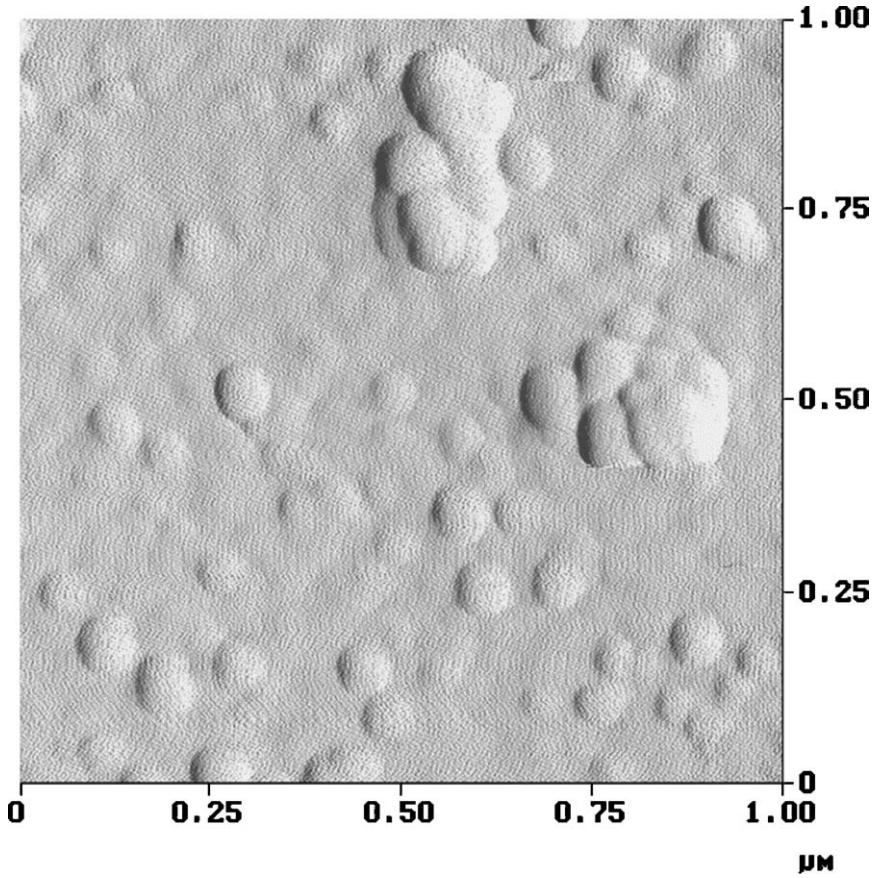

Fig. 3. AFM image of 40 nm MgO film deposited on 6 nm SrO buffer layer. RMS roughness is <2 nm. A 3D island growth mode is evident. The deflection image shown has a 1 nm z-range.

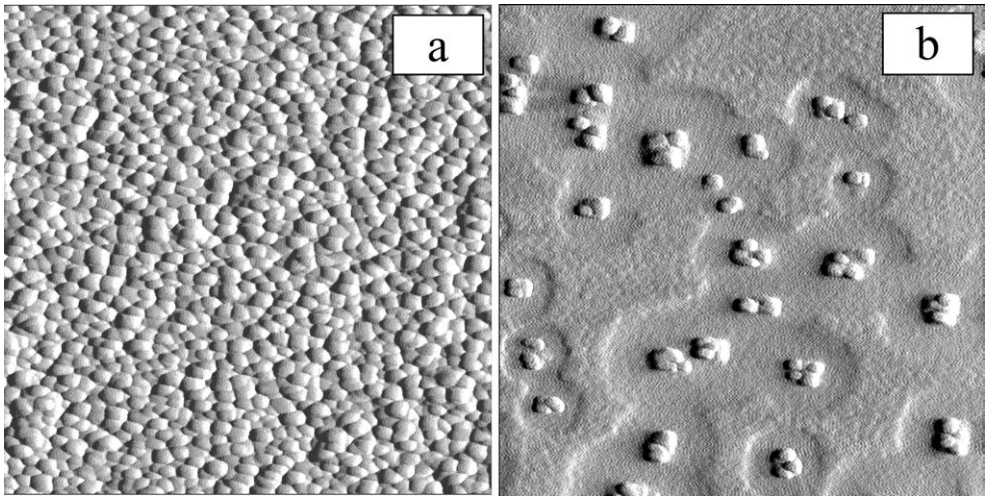

Fig. 4. AFM images of $SrTiO_3$ buffer layers grown (a) at 700°C and (b) by recrystallization with initial deposition at 200°C followed by an anoxic at 700°C. The film deposited at 700°C exhibits an island growth mode while that grown using the annealing method show a Stranski-Krastanov transition.

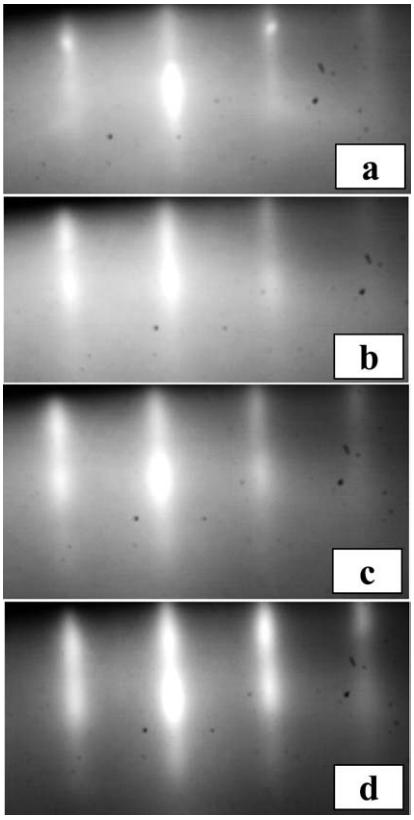

Fig. 5. RHEED patterns for four $SrTiO_3$ deposition and anneal cycles. (a) 1st cycle 5 Å 2D STO film, (b) 2nd cycle 10 Å STO film, (c) 3rd cycle 15 Å STO film, (d) 4th cycle 40 Å STO film.

subsequent deposition and anneal cycles indicate that the film evolves from a smooth 2D epitaxial film to a mixed 2D and 3D epitaxial film. Figure 4(b) shows an AFM image of the resultant 5.2 nm $SrTiO_3$ film with a mixed two dimensional and island growth morphology. The RHEED patterns for $SrTiO_3$ films on Si(001) prepared by both methods indicate a $SrTiO_3$ [100]||Si[110] orientation. Cross-sectional TEM of the $SrTiO_3$ film formed by recrystallization (Fig. 6) likewise indicates a $SrTiO_3$[100]||Si[110] orientation. X-ray diffraction analysis of the film indicates that it is phase pure with a single epitaxial orientation. From the θ–2θ peak positions of the $SrTiO_3(00l)$ peaks the lattice parameter was found to be 3.91 Å, which is comparable to the bulk value, indicating that the $SrTiO_3$ film is fully relaxed.

Epitaxial MgO was subsequently deposited on a $SrTiO_3$ buffer layer grown at 700°C. The RHEED patterns of both the $SrTiO_3$ buffer layer and the MgO film indicate an island growth mode with a MgO[100]||$SrTiO_3$[100] orientation. Efforts to deposit MgO on $SrTiO_3$ grown by recrystallization are under way. MgO deposition on $SrTiO_3$ grown by this method is expected to show a much improved surface morphology owing to the lower roughness of the buffer layer. Furthermore, as two-dimensional $SrTiO_3$ layers have been previously demonstrated by Li et al., continued improvements in the $SrTiO_3$ buffer layer morphology are expected [12].

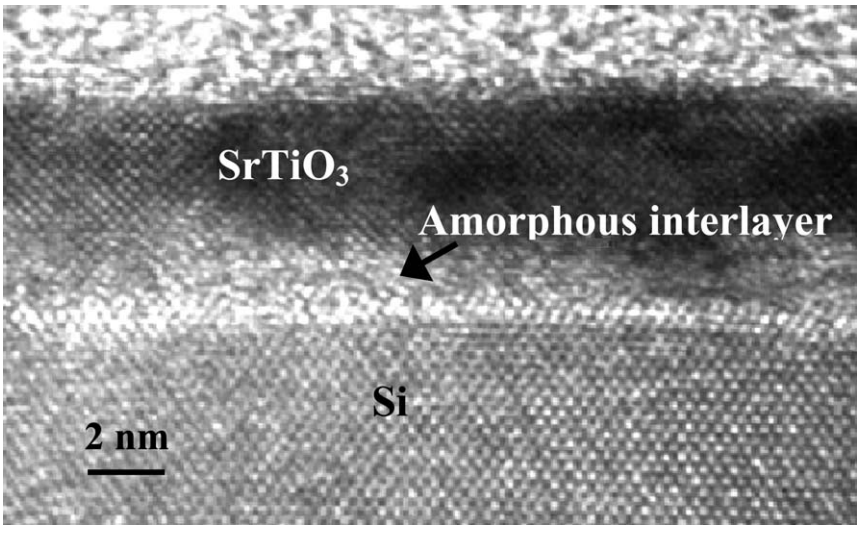

Fig. 6. Cross-sectional TEM of $SrTiO_3$ buffer layer on a Si substrate. SrTiO3 buffer layer was grown by the recrystallization method. An amorphous interlayer is evident. Cross-section is along the Si[110] direction and shows a $SrTiO_3$[100]Si[110] orientation for the film.

Conclusions

Heteroepitaxial MgO(001) oriented overlayers have been deposited on Si(001) substrates using both SrO and $SrTiO_3$buffer layers. The MgO orientation with a SrO buffer layer is Si[100]||SrO[100]||MgO[100]. For MgO on Si using SrO buffer layers, best results were achieved using a two step growth process with O_2 partial pressures of between 4×10^{-8} and 1.2×10^{-7} Torr on SrO buffer layers of at least 2.5 nm. XRD analysis indicated a MgO(002) rocking curve FWHM of 2.2°. Film morphology indicated an island growth mode with coalescence. Epitaxial $SrTiO_3$ buffer layers were deposited using a fixed stage temperature of 700°C as well as by recrystallization. Films grown by recrystallization were phase pure and exhibited an improved surface morphology due to a Stranski-Krastanov growth mode. X-ray analysis indicates the 5.2 nm $SrTiO_3$ film grown by recrystallization was fully relaxed. The MgO orientation with a $SrTiO_3$ buffer layer is Si[110]||STO[100]||MgO[100].

Acknowledgments

This work was supported by NSF ECS Grant 0123469, NSF MRSEC DMR-0076077, and MDA-STTR program through a subcontract from SVT Associates.

References

1. D.K. Fork, F.A. Ponce, J.C. Tramontana, and T.H. Geballe, *Applied Physics Letters*, **58**, 2294 (1991).
2. B.S. Kwak, E.P. Boyd, K. Zhang, A. Erbil, and B. Wilkins, *Applied Physics Letters*, **54**, 2542 (1989).
3. R. Huang and A.H. Kitai, *Applied Physics Letters*, **61**, 1450 (1992).
4. F. Niu, B.H. Hoerman, and B.W. Wessels, *Journal of Vacuum Science and Technology B*, **18**, 2146 (2000).
5. A.K. Sharma, A. Kvit, and J. Narayan, *Journal of Vacuum Science and Technology A*, **17**, 3393 (1999).
6. T. Tambo, T. Nakamura, K. Madeda, H. Ueba, and C. Tatsuyama, *Japanese Journal of Applied Physics*, **37**, 4454 (1998).
7. T. Tambo, A. Shimizu, A. Matsuda, and C. Tatsuyama, *Japanese Journal of Applied Physics*, **39**, 6432 (2000).
8. T. Higuchi, Y.Chen, J. Koike, S. Iwashita, M. Ishida, and T. Shimoda, *Japanese Journal of Applied Physics*, **41**, 6867 (2002).
9. G. Chern and C. Cheng, *Journal of Vacuum Science and Technology A*, **17**, 1097 (1999).
10. J. Lettieri, J.H. Haeni, and D.G. Schlom, *Journal of Vacuum Science and Technology A*, **20**, 1332 (2002).
11. R.A. McKee, F.J. Walker, and M.F. Crisholm, *Physical Review Letters*, **81**, 3014 (1998).
12. H. Li, X. Hu, Y. Wei, Z. Yu, X. Zhang, R. Droopad, A.A. Demkov, J. Edwards, Jr., K. Moore, W. Ooms, J. Kulik, and P. Fejes, *Journal of Applied Physics*, **93**, 4521 (2003).